SEMARAK ILMU PUBLISHING

Journal of Advanced Research in Fluid Mechanics and Thermal Sciences

Journal homepage:
https://semarakilmu.com.my/journals/index.php/fluid_mechanics_thermal_sciences/index
ISSN: 2289-7879

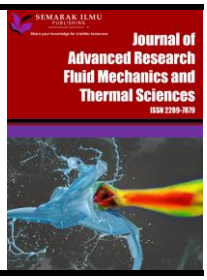

Analysis of Fluid Flow on the N95 Facepiece Filtration Layers

Muhammad Nur Hanafi Harolanuar[1], Nurul Fitriah Nasir[1,*], Hanis Zakaria[1], Ishkrizat Taib[1]

[1] Faculty of Mechanical and Manufacturing Engineering, Universiti Tun Hussein Onn Malaysia, 86400, Parit Raja, Batu Pahat, Johor, Malaysia

ARTICLE INFO

Article history:
Received 19 April 2022
Received in revised form 7 September 2022
Accepted 20 September 2022
Available online 11 October 2022

Keywords:
N95 facepiece; COVID-19 virus droplets; fluid flow analysis; filtration layers

ABSTRACT

Due to the general confusion over the mask's efficiency against COVID-19 virus droplets, professionals and the public may find it difficult to stop the disease from spreading. This study intends to investigate the fluid flow across the N95 filtration layer based on the experimental data and create a simulation model based on the analysis. Therefore, the fluid flow across the filtration layer is simulated using ANSYS Fluent, part of Computational Fluid Dynamics (CFD) solver software. This study anticipates the fluid flow across the N95 by using the porous media approach, in which inertial resistance and viscous resistance are introduced in the simulation by obtaining the pressure drop coefficient of the actual 3M N95 filtration. The fluid passed through the filtration layer with some velocity range based on the MS 2323:2010 standard. The pressure and velocity distribution of fluid through the filtration layer are analyzed by simulation illustration of the contour and streamline of the fluid. For most conditions, as fluid flowed across the filter, the flow gradually began to retard and diverge around the filtration layer. Besides, different flow rates across the filtration layer also result in different pressure distributions on the N95 layer. To sum up, this study is beneficial in forecasting the fluid behavior across the filtration layer by applying the porous zone approach in the ANSYS simulation.

1. Introduction

The severe acute respiratory syndrome coronavirus-2 (SARS-CoV-2) virus, which caused the Corona Virus Disease (COVID-19) pandemic, has shaken the world for the previous few years. This epidemic substantially influences the global community, affecting people's health and lives. This disease originated in Wuhan City, Hubei Province, Republic of China, and has spread worldwide, including Malaysia [1]. According to the weekly update of newly confirmed cases, this virus is highly contagious and deadly. As of the 21st Mac 2021, the cumulative issues of 122,536,880 and 2,703,780 die around the world [2]. Without a doubt, each country affected by the pandemic must adapt its strategy for dealing with virus transmission. However, WHO guidelines require that all humankind should be dealt with the airborne and contact precautions [3].

* *Corresponding author.*
E-mail address: fitriah@uthm.edu.my

https://doi.org/10.37934/arfmts.100.1.172180

The SARS-CoV-2 virus spreads by direct transmission (droplet and human-to-human) and indirect transmission when smaller droplets and particles can stay in the air for a long time from the droplet with the deadly virus [4]. In addition, people need to practice social distancing and wear masks to keep respiratory viral diseases to keep the COVID-19 disease from spreading. The masks help decrease virus transmission within the population by preventing anyone from spreading the infection to others, including those unknowingly infected [5]. Additionally, a well design ventilation will also help to improve air distribution thus preventing the virus spread [6].

The principle of liquid filtration may apply to airborne particle filtering as well. The fluid-particle behaves differently than the airborne particle since it is considerably larger. It may also be seen when water, as a representation of a liquid, cannot pass through the filtration layer, which works on the concept of airborne particle filtration. The user should be given breathable filtration of the surgical mask and respirator material during intake and exhale. Past research has shown that the filtration components mechanism consisting of electrostatic attraction, diffusion, interception, and inertial impaction are represented by the porous zone condition from the simulation [7].

A porous medium simulation studies the behaviour and movements of molecules and particles through packed beds, perforated plates, and filter sheets. The porous medium simulation by ANSYS Fluent involves the velocity, viscous, and inertial resistance from the Navier-Stokes equation with an additional pressure drop applied to the flow through the porous material [8]. The porous medium represents the filtration layer in this study so that the air streamline is utilized in a particular direction, i where the Darcy-Forcheimer equation is used in the ANSYS Fluent as the external body force term, as shown in Eq. (1).

$$\frac{\Delta p}{\Delta x_i} = -\frac{\mu}{\alpha} v_i + 0.5 \cdot C_2 \cdot \rho \cdot |v| \cdot v_i \tag{1}$$

The $1/\alpha$ and C_2 variables represent the viscous resistance and inertial resistance coefficient following the specific direction, i (direction of the air streamline through the filtration layer), based on the pressure drop of the porous medium. A pressure drop versus velocity parabolic graph should be constructed, and the function can be written by comparing two equations: Eq. (1) and Eq. (2). While the viscous resistance, $1/\alpha$ and inertial resistance, C_2 coefficient (Eq. (3) and Eq. (4)) can be calculated. Where the Δx is the filtration layer (porous material) parallel to the direction of the air streamline, ρ, and μ represent the density and the viscosity of the fluid flow.

$$\Delta p = a v_i^2 + b v_i + c \tag{2}$$

$$\frac{1}{\alpha} = \frac{b}{\mu \cdot \Delta x} \tag{3}$$

$$C_2 = \frac{2a}{\rho \cdot \Delta x} \tag{4}$$

After all, the misunderstanding over the mask's effectiveness against COVID-19 virus droplets may make it difficult for professionals and the public to stop the virus from spreading. While the present method of studying and investigating the filter layer's efficiency is mostly through powered randomized controlled trials (RCTs) and experimental techniques, this is time-consuming and must be carried out in a controlled setting [9]. In this study, the fluid flow behaviour across the filter layer of the respirator against the Covid-19 droplet virus or aerosol is investigated. Besides, Solidworks is

used to generate the geometrical representation of the filtration layer for the simulation and findings, and the ANSYS Fluent is the simulation platform.

2. Methodology

This study used the ANSYS Fluent as the Computational Fluid Dynamics (CFD) Solver to predict the fluid flow behaviour across the N95 filtration layer. The simulation setup is based on the MS 2323:2010 standard that replicates the user's breathing condition while wearing the face mask [10]. The simulation study consists of the porous medium geometry design using Solidworks software and the fluid flow simulation using ANSYS Workbench. Before running the simulation, Solidworks defines the fluid domain and filtration layer. In Solidworks, each part is modeled independently and assembled, consisting of several layers based on the patent designed by the United States Patent [11]. In addition, opened and closed conditions of the fluid flow are introduced for the simulation to differentiate the flow of air during experimental and open surroundings. Before proceeding to the ANSYS Fluent simulation, the analysis of the porous zone, including the inertial and viscous resistance, should be considered at the beginning by using the filter pressure drop coefficient and Eq. (3) and Eq. (4). The simulation consists of three parts: pre-processing, processing, and post-processing.

The geometry, including the filtration layer and the fluid domain geometry, is then saved to the ACIS, STEP, or Parasolid file before being imported to the ANSYS Fluent platform. If any mistakes were made during the drawing in SolidWorks, ANSYS Design Modeler is used to verify that they were fixed before mesh generation and FLUENT settings could be applied.

Next, the meshing of the modified geometry takes place, which can only be done once the geometric input is complete. The Finite Element Method, or in this case, ANSYS, may solve a persistent problem through a process known as meshing. Meshing was used to divide the domain into pieces, representing an element [12]. The focal area at the meshing configuration is the porous zone component, and the surrounding fluid domain is then selected using the sizing approach for meshing mode analysis.

For the system to recognize default boundary conditions, named selections are required. The inlet, outlet, wall, and filtration layer as the porous zone are then identified for the study's boundary condition, as shown in Figure 1. The FLUENT settings utilized in this study are shown in Table 1. For this simulation, only the highest and lowest inlet velocity were used by comparing with open and closed conditions. The flowrate was chosen for simulation was referred to TSI Automated Filter Tester 80130A based on a normal person's activity.

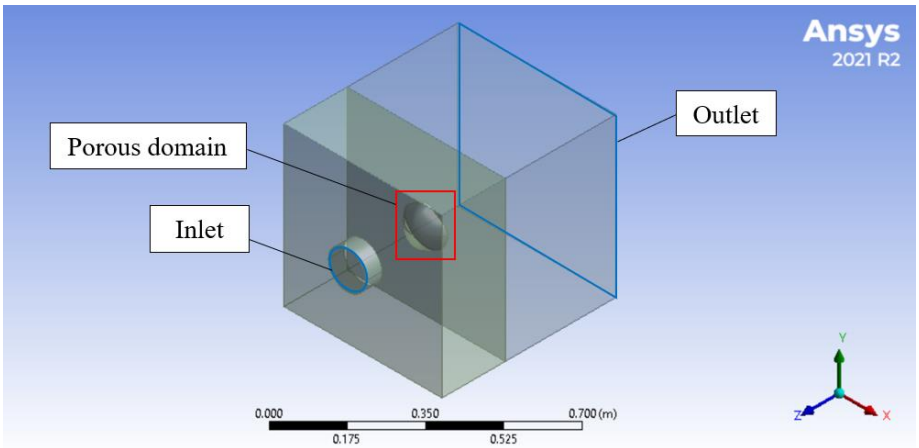

Fig. 1. Inlet, Outlet, Porous and non-porous domain

Table 1
ANSYS Fluent configuration setting

Solver setting	
Dimension	3-Dimensional
Processing option	Parallel (8 processes local machine)
General analysis solver	
Solver type	Pressure-based
Velocity formulation	Absolute
Time	Steady
Model Setup	
Viscous model	K-epsilon (K-ε), 2 equations
K-epsilon model	Standard
Cell Zone Conditions (Filter Domain)	
Porous Zone	Direction-1 vector $(x = 1, y = 0, z = 0)$ Direction-2 vector $(x = 1, y = 0, z = 0)$
Fluid Material	Air
Boundary Conditions	
Inlet	Velocity Magnitude: 0.035 m/s and 0.011 m/s Initial Gauge pressure: 0 Pa Turbulence Specification method: Intensity and Viscosity Ratio Turbulence Intensity: 5%
Outlet	Gauge pressure: 0 Pa Turbulence Specification method: Intensity and Viscosity Ratio Turbulence Intensity: 5% Turbulence Ratio: 10
Wall	Wall motion: Stationary wall Shear condition: No-slip Wall roughness: Standard model Prevent backflow

Another vital part of the study is knowing the pressure drop across the N95 filtration layer using the TSI Automated Filter Tester 80130A. The equipment is among the most acceptable options for evaluating particle respirator filters, disposable filtering facepieces, and various filter media. Materials involved in this experiment are the N95 as the sample, a hot glue gun to provide the adhesive to the sample, and the steel plate to hold the sample. All previously provided parameters were put into action on the setup during the processing steps. This stage is required to be perfect for the results to be significant.

3. Results and Discussion

3.1 Grid Independence Test

The mesh size had to be adjusted four times before velocity measurements could be taken to obtain the correct elements. Re-meshing pieces can determine the correct mesh size into smaller sizes. The measure was re-meshed throughout the fluid domain by altering the element size. An element size of 25 mm is the most suitable size for the study's geometry. This could be proven that the average velocity across the filtration layer shows the lowest relative error at 0.409% and confirm that it was an excellent meshing. The meshing quality of the geometry shows in the range of the acceptance for the skewness and the orthogonal quality, as shown in Table 2.

Table 2
Results of Grid Independence Test

Test	Element size (mm)	No. of nodes	No. of elements	Average skewness	Average orthogonal	Average velocity (m/s)	Relative error %
1	29	14462	74242	0.24428	0.75489	0.012055	0.937
2	27	15305	78732	0.24344	0.75577	0.011942	1.407
3	25	16634	85731	0.2427	0.75649	0.011774	0.409
4	23	18513	95102	0.24198	0.75714	0.011726	0.506

3.2 Cell Zone Condition

Before introducing the input to the cell zone condition, or more specifically, the filter domain, some analysis was carried out, particularly for the viscous and inertial resistance of the cell zone. Nevertheless, the filter pressure drop coefficient parameter was obtained from the TSI Automated Filter Tester. The N95 filter's pressure drop coefficient is critical for determining the N95's viscous and inertial resistance. The results of the pressure drop were in mmH_2O unit and then converted to Pascals by using Eq. (5), where the density of water, $\rho = 997\ \mathrm{kg/m^3}$ and the gravitational force, $g = 9.81\ \mathrm{m/s}$, as shown in Table 3. The pressure drop coefficient could be calculated from the pressure drop using the polynomial graph, as shown in Figure 2. Different materials, fluids, dimensions, and conditions result in different pressure drop coefficients and viscous and inertial resistance based on the heat sink study [13]. Based on the graph obtained, the pressure drop coefficient of the N95 filtration layer is $\Delta P = 50352v^2 + 188.05v + 20.055$.

$$P = \rho g h \tag{5}$$

The results of viscous and inertial resistance are summarized in Table 4. Once those values have been acquired, the cell zone condition includes the viscous and inertial resistance obtained, which are 39205670.80 $(1/m^2)$ and 31020408.16 $(1/m)$, which were put in the simulation. Only the z-axis, or the third direction for the simulation, must be included in the cell zone condition.

Table 3
The pressure drops across the N95 filtration layer

Flowrate (L/min)	Velocity (m/s)	TSI result, (mmh_2O)	Pressure drop, ΔP (Pa)
30	0.0111	2.87	28.07
55	0.02	4.60	44.99
68	0.025	5.72	55.94
82	0.03	7.16	70.03
95	0.035	9.09	88.91

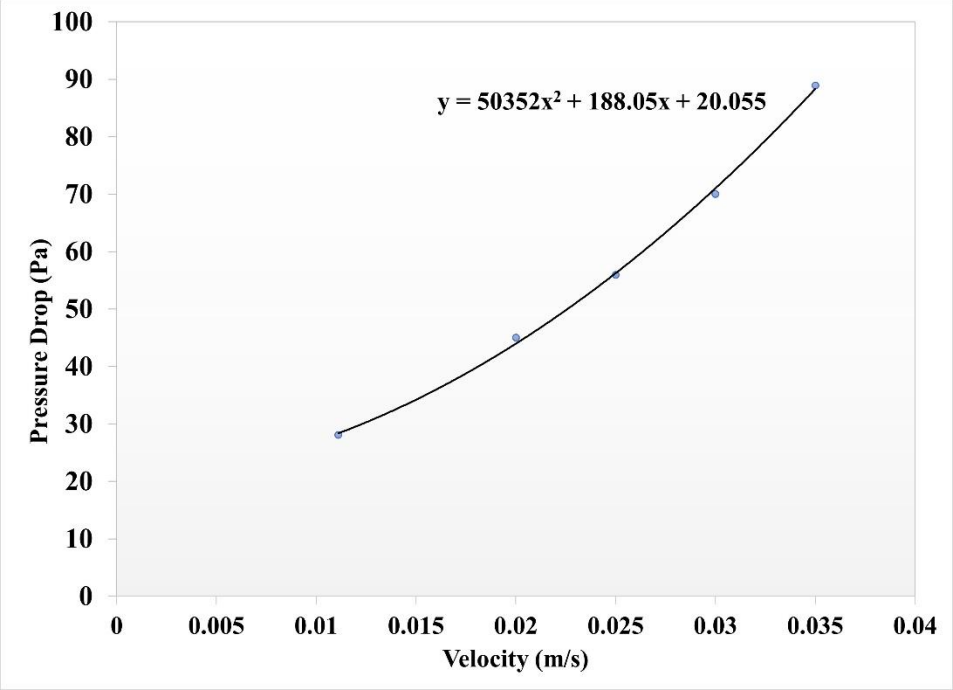

Fig. 2. N95 Filter Pressure Drop Coefficient

Table 4
Inertial and Viscous Resistance of the N95 respirator

$\Delta p = av_i^2 + bv_i + c$ $\Delta P = 50352v^2 + 188.05v + 20.055$	
a coefficient	50350
b coefficient	188.05
Filter thickness (m)	0.00265
Density(kg/m^3)	1.225
Viscosity $(kg/m.s)$	0.00181
Inertial resistance $(1/m)$	31020408.16
Viscous resistance $(1/m^2)$	39205670.80

3.3 Velocity and Pressure Distribution Across the Filtration Layer

For most conditions, as fluid flowed across the filter, the velocity at 0.035 m/s of the flow gradually began to retard and diverge around the filtration layer. The reason is that the inertial and viscous resistance of the filter is high enough to prevent the air passed through, whereas Figure 3(a) and (b) illustrate the fluid behavior. For the closed condition, although there is a wall presence around the filtration layer, the air could pass through as shown in Figure 3(b) and Figure 3(d) of the velocity streamline because of the porous zone, which is the filtration layer. When the velocity is at 0.011 m/s, the velocity contour is the same as the 0.035 m/s, but the only difference is the flow's distance could travel.

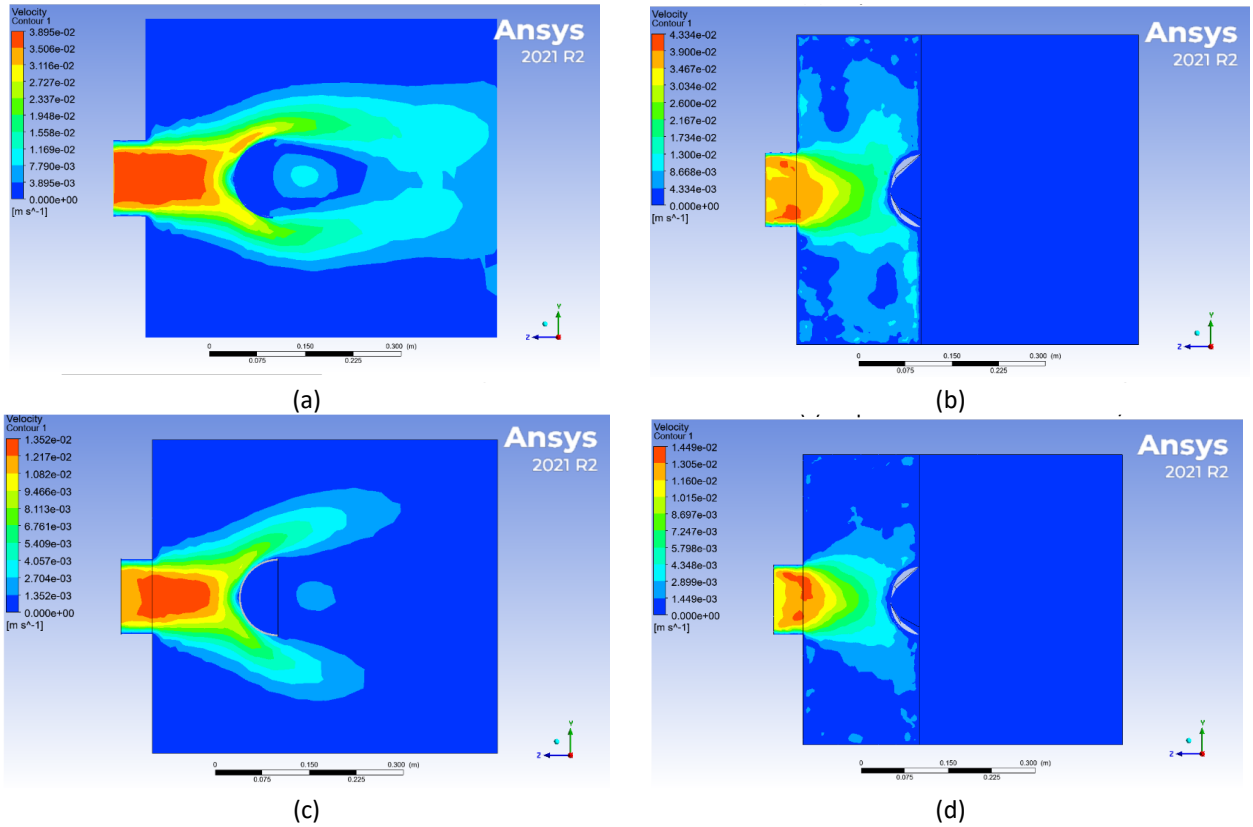

Fig. 3. Velocity distribution across the filtration layer; (a) Open condition at V = 0.035 m/s, (b) Closed condition at V = 0.035 m/s, (c) Open condition at V = 0.011 m/s, (d) Closed condition at V = 0.011 m/s

Figure 4 shows that pressure distribution was affected by the velocity. From the simulation, different velocity ranges might result in various locations for the filtration location. For instance, in the pressure distribution at the 0.035 m/s velocity condition, fluid flow pressure is focused on the top left of the filtration layer, as illustrated in Figure 4(a). The pressure distribution did not occur toward the centre of the respirator but was significant around the tip of the respirator. This may be caused by the leakage around the respirator. In comparison, the pressure distribution at 0.011 m/s shows that the air focused on the middle of the N95 filtration layer, as shown in Figure 4(b). A uniform pressure distribution was found for inlet velocity at 0.011 m/s, and the pressure decreased when the air moved away from the nose. Previous research also confirmed that as the air flows around the tip of the respirator, separation will occur toward the center of the channel [14].

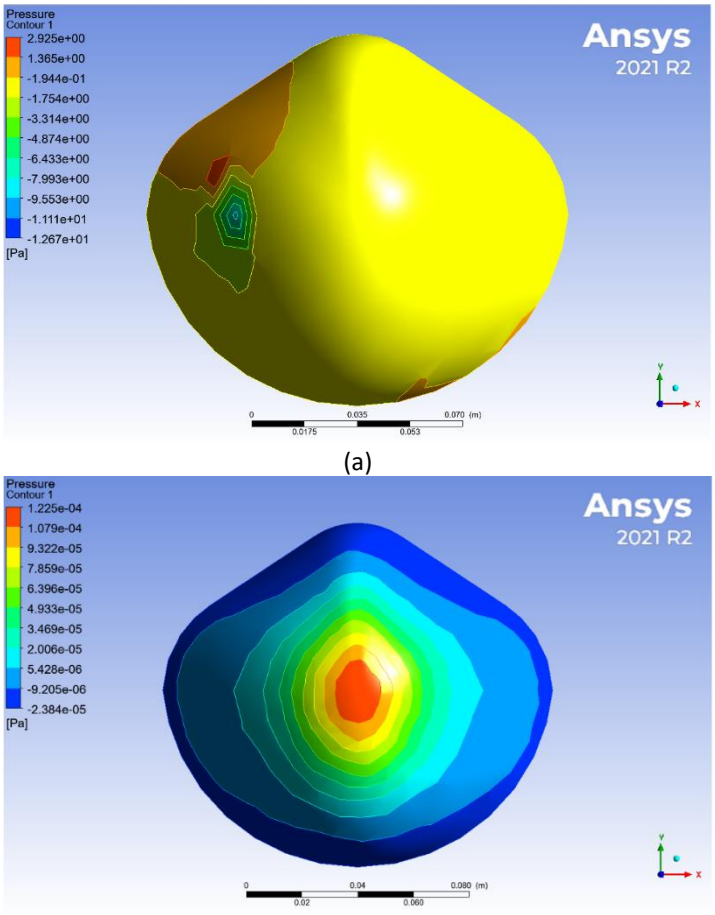

Fig. 4. Pressure Contour on the filtration layer; Contour of filtration layer at (a) 0.035 m/s, (b) 0.011 m/s

4. Conclusions

The fluid flow behavior across the filter layer of the respirator against the Covid-19 droplet virus or aerosol has been investigated. From the results of pressure simulation on the filtration layer, they have shown the specific region where the droplets accumulate. The lower velocity simulation resulted in the pressure focused on the middle of the N95 filtration layer. In contrast, at the high velocity, the pressure contour concentrates at the tip of the N95 mask. This simulation helps to add knowledge on the velocity and pressure distribution for the N95, and different geometry might result in various pressure contours on the filtration layer. This simulation also proves that the N95 particulate respirator with an exhalation valve in the center is not suitable to protect from virus COVID-19 especially.

Acknowledgement

The authors wish to acknowledge the Research Management Centre, Universiti Tun Hussein Onn Malaysia, for their financial support of this research work under Grant TIER 1 Vote Number H861. A special appreciation to Mr. Baderin Osman from Consultation, Research and Development Department, National Institute of Occupational Safety and Health Malaysia, for his continuous research support.

References

[1] Cheng, Shao-Chung, Yuan-Chia Chang, Yu-Long Fan Chiang, Yu-Chan Chien, Mingte Cheng, Chin-Hua Yang, Chia-Husn Huang, and Yuan-Nian Hsu. "First case of Coronavirus Disease 2019 (COVID-19) pneumonia in Taiwan." *Journal of the Formosan Medical Association* 119, no. 3 (2020): 747-751. https://doi.org/10.1016/j.jfma.2020.02.007

[2] World Health Organization. "COVID-19 Weekly Epidemiological Update." *WHO*. November 15, 2020. https://www.who.int/docs/default-source/coronaviruse/situation-reports/weekly-epi-update-14.pdf.

[3] Van Doremalen, Neeltje, Trenton Bushmaker, Dylan H. Morris, Myndi G. Holbrook, Amandine Gamble, Brandi N. Williamson, Azaibi Tamin et al. "Aerosol and surface stability of SARS-CoV-2 as compared with SARS-CoV-1." *New England Journal of Medicine* 382, no. 16 (2020): 1564-1567. https://doi.org/10.1056/NEJMc2004973

[4] Lotfi, Melika, Michael R. Hamblin, and Nima Rezaei. "COVID-19: Transmission, prevention, and potential therapeutic opportunities." *Clinica Chimica Acta* 508 (2020): 254-266. https://doi.org/10.1016/j.cca.2020.05.044

[5] Eikenberry, Steffen E., Marina Mancuso, Enahoro Iboi, Tin Phan, Keenan Eikenberry, Yang Kuang, Eric Kostelich, and Abba B. Gumel. "To mask or not to mask: Modeling the potential for face mask use by the general public to curtail the COVID-19 pandemic." *Infectious Disease Modelling* 5 (2020): 293-308. https://doi.org/10.1016/j.idm.2020.04.001

[6] Hatif, Ihab Hasan, Azian Hariri, and Ahmad Fu'ad Idris. "CFD analysis on effect of air Inlet and outlet location on air distribution and thermal comfort in small office." *CFD Letters* 12, no. 3 (2020): 66-77. https://doi.org/10.37934/cfdl.12.3.6677

[7] Institute of Medicine of the National Academies. *Reusability of Facemasks During an Influenza Pandemic: Facing the Flu*. National Academies Press, 2006.

[8] Wang, Yuan, Matthew Brannock, Shane Cox, and Greg Leslie. "CFD simulations of membrane filtration zone in a submerged hollow fibre membrane bioreactor using a porous media approach." *Journal of Membrane Science* 363, no. 1-2 (2010): 57-66. https://doi.org/10.1016/j.memsci.2010.07.008

[9] Howard, Jeremy, Austin Huang, Zhiyuan Li, Zeynep Tufekci, Vladimir Zdimal, Helene-Mari van der Westhuizen, Arne von Delft et al. "An evidence review of face masks against COVID-19." *Proceedings of the National Academy of Sciences* 118, no. 4 (2021): e2014564118. https://doi.org/10.1073/pnas.2014564118

[10] British Standard. "Respiratory Protective Devices. Filtering Half Masks to Protect Against Particles-Requirements, Testing, Marking." *BS EN 149:2001+A1:2009*. BSI, 2001.

[11] Daugaard, Dwayne D., Daniel J. Stepan, Yonas Gebrewold, Michael K. Domroese, and Lance E. Behymer. "Filtering face-piece respirator having nose clip molded into the mask body." *U.S. Patent 8,066,006*, issued November 29, 2011.

[12] Ozen, Metin. "Meshing workshop." *Ozen Engineering*, 2014.

[13] Nowak, Remigiusz. "Estimation of viscous and inertial resistance coefficients for various heat sink configurations." *Procedia Engineering* 157 (2016): 122-130. https://doi.org/10.1016/j.proeng.2016.08.347

[14] Hariharan, Prasanna, Neha Sharma, Suvajyoti Guha, Rupak K. Banerjee, Gavin D'Souza, and Matthew R. Myers. "A computational model for predicting changes in infection dynamics due to leakage through N95 respirators." *Scientific Reports* 11, no. 1 (2021): 1-19. https://doi.org/10.1038/s41598-021-89604-7